Lateral Mobility of Tethered Vesicle−DNA Assemblies

J. J. Benkoski[†] and F. Höök*[,‡]

Applied Physics Department, Chalmers University of Technology, Gothenburg, Sweden, and Solid State Physics Department, Lund University, Lund, Sweden

Received: November 4, 2004

Supported lipid membranes are particularly attractive for use in biochemical assays because of their resistance to nonspecific adsorption and their unique ability to host transmembrane proteins. Although ideal for use in many surface-based detection techniques, supported bilayers can make the incorporation of proteins problematic due to the steric constraints of the underlying substrate. A recently developed strategy overcomes this obstacle by tethering liposomes to supported lipid bilayers via cholesterol-tagged DNA. Due to the fluidity of the bilayer, the vesicle assemblies exhibited significant lateral mobility. The corresponding diffusion coefficients were then investigated using fluorescence recovery after photobleaching (FRAP). The diffusivity was neither sensitive to the size of the vesicles nor to the length of the DNA tether. However, changing from single cholesterol tethers to double cholesterol tethers caused a decrease in the diffusivity of the assemblies by a factor of 3. Perhaps even more notable was the fact that single cholesterol−DNA without vesicles diffused 6 times faster than the corresponding assemblies. Double cholesterol−DNA diffused 11 times faster. This discrepancy is believed to arise from the fact that each vesicle is tethered to the bilayer by multiple DNA pairs.

Introduction

Supported Lipid Bilayers. Supported phospholipid bilayers (SPBs) are particularly attractive for use in biochemical assays because of their resistance to nonspecific binding and their ability to host biologically active molecules, such as antibodies, water-soluble proteins, and DNA.[1−3] Perhaps most important is their unique ability to host transmembrane proteins.[4,5] Though not as durable as grafted polymer chains, SPBs tend to be more biologically inert. Their superior biocompatibility arises from the similarity of their mobility, local electrostatics, hydration shell, and elasticity to that of a cell membrane. Such properties are key to preserving both the selectivity and biological activity of the sensor element. As a surface-bound structure, the SPB has the further advantage of compatibility with a variety of surface-based detection techniques. Quartz crystal microbalance (QCM),[6] surface plasmon resonance (SPR),[7,8] fluorescence microscopy,[9] surface acoustic wave (SAW),[10] the surface force apparatus (SFA),[11] and atomic force microscopy (AFM)[12] are just a few of the techniques that can be used in conjunction with biofunctionalized SPBs.

One drawback of the SPB is the fact that the steric constraint of the underlying substrate can make the incorporation of transmembrane proteins problematic.[4] In addition to hampering bilayer formation, the embedded proteins within the SPB have also been observed to exhibit reduced mobility.[13] Such effects have necessitated more advanced solutions that involve various spacers between the lipid layer and substrate.[14,15] A lipid structure which does not suffer from such constraints is the small unilamellar vesicle (SUV) suspended in aqueous solution. The incorporation of transmembrane proteins into SUVs is routinely accomplished by detergent-mediated reconstitution.[16] In this method, the proteins are mixed with a detergent in the presence of liposomes. Upon dilution of the suspension, the proteins become spontaneously incorporated into the vesicles. Although SUV suspensions provide the easiest and most direct route for the incorporation of transmembrane proteins, they are incompatible with surface-based detection techniques. This inability to directly monitor events on the vesicle surfaces places strong constraints on the detection of biological activity. The best solution is therefore one that can combine the strengths of the two geometries.

Tethered Vesicles. A recently developed strategy achieves this combination by tethering liposomes to supported lipid bilayers via cholesterol-tagged DNA. As illustrated in Figure 1, the DNA tether is formed by first adding the cholesterol−DNA to the solution in contact with the supported lipid bilayer. The cholesterol then spontaneously embeds itself within the hydrophobic interior of the bilayer, forming a mobile anchor. Finally, a suspension of vesicles decorated with the complementary cholesterol−DNA is added, and the DNA pairs hybridize to complete the assembly.

Since the coupling of cholesterol to the hydrophobic interior involves only noncovalent chemistry, it has several advantages over corresponding methods that involve functionalized lipids. These include faster coupling rates, removing the need for functionalized lipids, and eliminating unintended side reactions between the lipid functional groups and the other membrane constituents.

The lateral mobility of such assemblies opens up many possibilities for their utilization in sensor and separation devices. On one hand, the vesicles can be tracked and eventually steered on an individual basis. Changes in the mobility of a single vesicle can then be used to monitor discrete recognition events or other biological processes. Also created are opportunities for mixing different types of functionalized vesicles on the surface followed by separation with respect to size or charge. The lateral

* To whom correspondence should be addressed. E-mail: fredrik.hook@ftf.lth.se.
[†] Chalmers University of Technology.
[‡] Lund University.

10.1021/jp044947p CCC: $30.25
Published on Web 04/15/2005

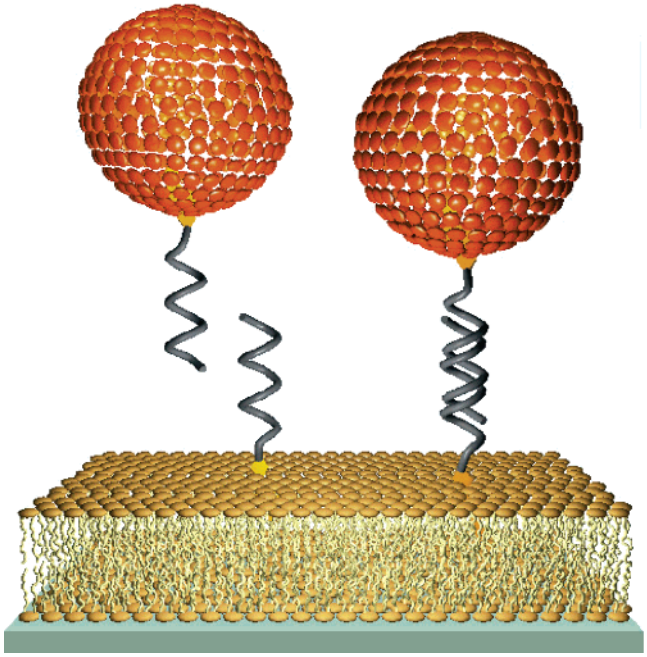

Figure 1. Illustration of tethered vesicle-DNA assembly, showing how the hybridization of complementary cholesterol-DNA pairs forms the mobile tether. The vesicles were doped with 1 wt % rhodamine−DHPE for direct observation by fluorescence microscopy.

mobility also opens up the freedom needed to control the formation of two-dimensional self-assemblies. On the other hand, lateral mobility can be a disadvantage when a permanent pattern or array is desired. Such patterning would require externally triggered means to control the detailed features of the design.

The above applications clearly motivate the need for understanding how lateral mobility may be controlled. Previous studies have reported results for vesicles tethered via lipid-functionalized DNA.[17,18] Whereas Patolsky et al. used the concept for signal amplification purposes, Yoshina-Ishii et al.[17] used single particle tracking to determine the diffusion coefficient of their assemblies. They recorded an average value of 0.9 $\mu m^2/s$, slower than but comparable to that observed for lipids in an SPB. In the current study, we perform a systematic study of the factors that control the diffusivity of vesicle−DNA assemblies anchored with cholesterol tags. These include the effects of vesicle size, tether length, and anchor size as measured by fluorescence recovery after photobleaching (FRAP).

Experimental Section

Vesicle Formation. Lipid vesicles were prepared according to the method of MacDonald et al.[19] by first dissolving 5 mg of 1-palmitoyl-2-oleoyl-sn-glycero-phosphocholine (POPC) in 1 mL of chloroform. Next, the solvent was evaporated under nitrogen to form a thin film along the walls of a round-bottom flask. A total of 1 mL of buffer containing 100 mM NaCl and 10 mM tris(hydroxymethyl)aminomethane (TRIS) with a pH of 8 was then added to the flask, and the contents were stirred until dissolved. Finally, the mixture was passed 11 times through a lipid vesicle extruder (Avanti Polar Lipids, Inc.) to form small unilamellar vesicles (SUVs). The pore size of the filter controlled the vesicle size, which was checked by a BI-90 Particle Sizer (Brookhaven Instruments Corporation). 30, 50, and 100 nm filters produced vesicles with mean diameters of 35, 70, and 110 nm, respectively. The polydispersity index was narrow and generally resided near 1.2.

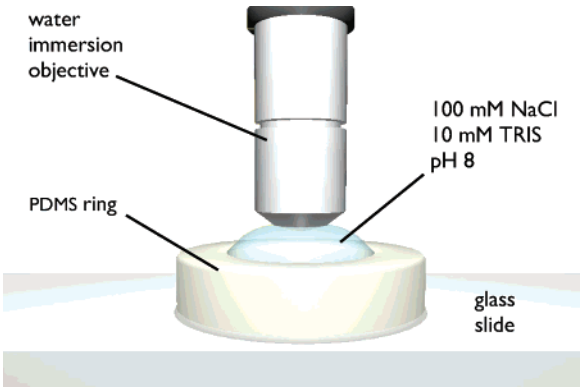

Figure 2. A PDMS ring placed atop a glass slide defined the sample volume. Approximately 1 mL of buffer was contained by the ring, and the fluorescent lipids on the surface were observed with a 40× water immersion objective.

Bilayer Formation. Supported lipid bilayers were formed upon glass slides. To clean the surfaces, the slides were exposed to a piranha treatment (3:1 sulfuric acid:30% hydrogen peroxide) for 30 min. A poly(dimethylsiloxane) (PDMS) ring placed in contact with the glass slide formed the sample cell, the walls of which confined the buffer to a volume measuring 17.5 mm in diameter and 4.0 mm in height, as shown in Figure 2. To this volume was added a 0.25 mg/mL suspension of 35 nm POPC vesicles. After waiting 30 min for bilayer formation, the suspension was exchanged with pure buffer.

Assembly Formation. Assembly formation proceeded with the addition of 3 μL of 20 μM cholesterol−DNA solution ($cDNA_{15}$, MedProbe Sweden) to 1 mL of TRIS buffer in the PDMS sample cell, giving a total concentration of 60 nM. Prepared in a TE buffer (10 mM TRIS, 1 mM ethylenediaminetetraacetate), $cDNA_{15}$ had the sequence shown in Table 1. 3 μL of a 20 μM solution of the complementary cholesterol−DNA ($cDNA_{15}'$, Table 1) was concurrently added to a vial containing 1 mL of a 0.20 mg/mL vesicle suspension. The two mixtures were then given a waiting time of 10 min to allow for the incorporation of the cholesterol tags into the lipid bilayers. With both processes complete, the suspension of vesicles decorated with the $cDNA_{15}'$ was added to the PDMS sample cell. The mixture was then allowed to stand for 10 min for the DNA hybridization to complete. Finally, the excess vesicles were removed by exchanging back to pure buffer.

FRAP. Fluorescence microscopy could be used to image either the tethered vesicles or the SPB through the addition of lissamine rhodamine B 1,2-dihexadecanoyl-sn-glycero-3-phosphaditylethanolamine (rhodamine-DHPE, $\lambda_{exc/em}$ = 550/590 nm, Molecular Probes, The Netherlands). To obtain the necessary fluorescence intensity, the POPC bilayer was doped with 0.5 wt % rhodamine−DHPE whereas the tethered POPC vesicles were modified with 1 wt % rhodamine−DHPE. The cholesterol−DNA anchors were also imaged with fluorescent labeling. For these measurements, the target cholesterol−DNA oligomers were hybridized with a rhodamine-modified complementary strand ($rDNA_{15}'$, Table 1). All measurements were performed on a Zeiss Axioplan 2 fluorescence microscope using a 40x water immersion objective.

All diffusivity measurements reported in this study were obtained by fluorescence recovery after photobleaching (FRAP).[20] This widely used technique is performed by first bleaching a small spot on a fluorescent surface. Unbleached molecules adjacent to the spot diffuse inward, leading to a recovery of the

TABLE 1: List of DNA Sequences Used in This Study

name	sequence	functional group
$cDNA_{15}$	5′-TGG-ACA-TCA-GAA-ATA-CCC−CC-3′	3′ cholesterol
$cDNA_{15}'$	5′-TAT-TTC-TGA-TGT-CCA-CCC−CC-3′	3′ cholesterol
$cDNA_{30}$	5′-GAA-CTC-GTG-GCT-TGG-ACA-TCA-GAA-ATA-CCC-3′	3′ cholesterol
$cDNA_{30}'$	5′-TAT-TTC-TGA-TGT-CCA-AGC−CAC-GAG-TTC−CCC-3′	3′ cholesterol
$dcDNA_{12}$	5′-CCC-GAA-CTC-GTG-GCT-3′	5′ cholesterol
$dcDNA_{30}$	5′-TGG-ACA-TCA-GAA-ATA-AGG-CAC-GAC-GGA-CCC-3′	3′ cholesterol
$dcDNA_{12}'$	5′-CCC-TCC-GTC-GTG-CCT-3′	5′ cholesterol
$rDNA_{15}'$	5′-TAT-TTC-TGA-TGT-CCA-CCC−CC-3′	5′ rhodamine

fluorescence within the spot. The characteristic time for fluorescence recovery (τ_D) varies as the square of the radius of the photobleached spot (w)

$$\tau_D = w^2/4D \tag{1}$$

where D is the diffusion coefficient.

The data analysis was performed according to the method of Ross, et al.[21] First, the data were collected from 31 time-lapse images collected over 30 s intervals. Both the spot radius and intensity profiles were then obtained using Scion Image on a Macintosh computer. After importing into Igor Pro, each intensity profile was fitted to a Gaussian function

$$y = a + b\exp[-(x-c)^2/2d^2] \tag{2}$$

where a is the vertical offset, b is the amplitude, c is the horizontal offset, and d is the standard deviation. Next, b was plotted as a function of time and was fitted to an exponential decay of the form

$$b = k + m\exp[-t/\tau_D] \tag{3}$$

Here k is the vertical offset, m is the amplitude, and τ_D is the characteristic time for recovery.

Results

Vesicle Size. The diffusivity of the vesicle assemblies was measured as a function of vesicle size, tether length, and anchor size. Typical FRAP micrographs are shown in Figure 3. Observe that the surface concentration was kept relatively high in order to minimize the graininess of the intensity profile. Although the concentration of vesicles was not entirely uniform across the surface, it was held essentially constant for each measurement by choosing locations that provided an autoexposure time of 500 ms. A series of such intensity profiles for 100 nm vesicles is given in Figure 4a. Note that the depth of the bleached well decreases progressively with each frame. Accordingly, the coefficients of the Gaussian fits decay exponentially with time, as shown in Figure 4b. The reported values were obtained from an average of 10 measurements performed on at least two different samples. The standard deviation was then reported as the error.

Figure 5 displays the diffusion coefficient as a function of vesicle size. The tethers for each test were assembled from hybridized $cDNA_{15}/cDNA_{15}'$ pairs. Note that all values are roughly equal to 0.3 $\mu m^2/s$ independent of vesicle size. The dotted line represents the diffusivity of a pure POPC bilayer, measured to be 0.85 $\mu m^2/s$. Also included in Figure 5 are the calculated diffusion coefficients for free vesicles in solution according to the Einstein relation[22]

$$D = \frac{k_B T}{6\pi\eta a} \tag{4}$$

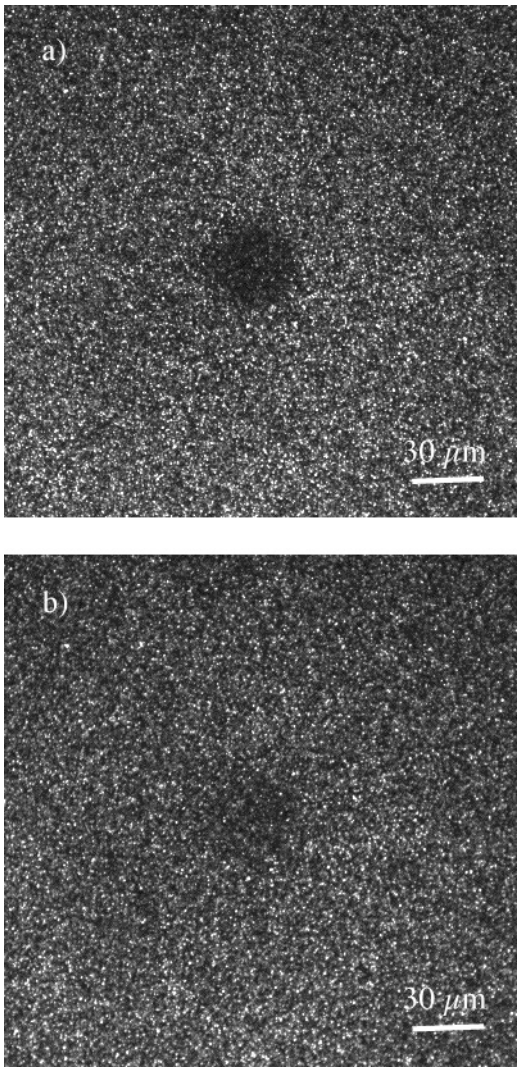

Figure 3. Typical micrographs showing a bleached spot in a field of 100 nm vesicles (a) immediately after bleaching and (b) after 5 min.

where k_B is Boltzmann's constant, T is the temperature (298 K), η is the viscosity of water (0.8904×10^{-3} Ns/m^2),[23] and a is the vesicle radius.

Tether Size. The tether length was increased from 15 mers to 30 by replacing $cDNA_{15}/cDNA_{15}'$ pairs with $cDNA_{30}/cDNA_{30}'$ hybridized pairs (Table 1). As seen in Figure 6, the diffusion coefficient was unchanged when measured for 110 nm vesicles.

Anchor Size. The anchor size was also modified after the method of Pfeiffer and Höök[24] by using the DNA assembly shown in Figure 7. For this tether, a 30 mer DNA with a cholesterol at the 3′ end ($cDNA_{30}'$, Table 1) was coupled with a 15 mer DNA with a cholesterol at the 5′ end ($dcDNA_{15}$, Table 1) such that both cholesterol tags were adjacent to each other. A third cholesterol−DNA strand ($cDNA_{15}$, Table 1) with its

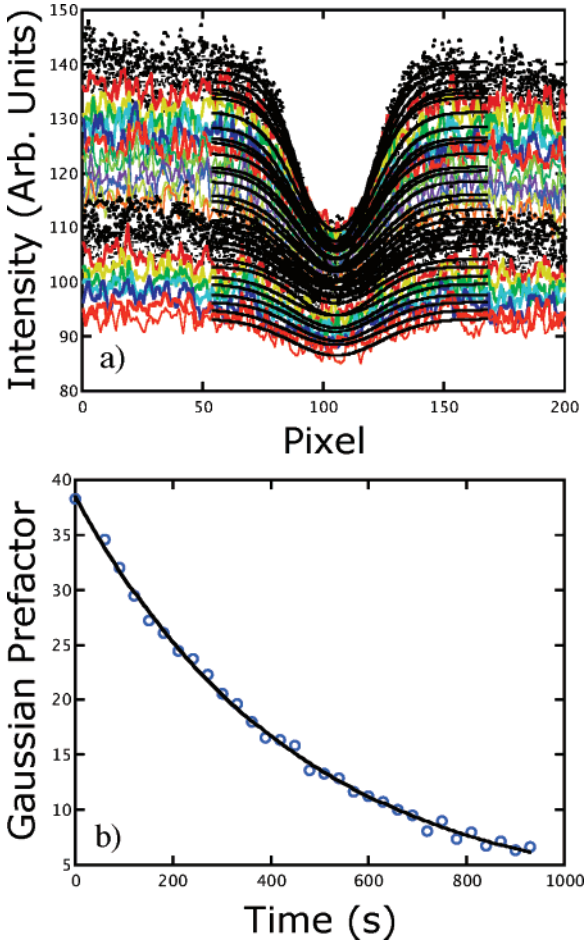

Figure 4. (a) Plot of successive intensity profiles for 100 nm vesicle−DNA assemblies. Here the experimental data is given by the various colored lines and the Gaussian fits are given by the solid black lines. (b) The fitting coefficients of the Gaussian are plotted as circles versus elapsed time. The exponential fit, given by a solid black line, was then used to calculate the diffusion coefficient.

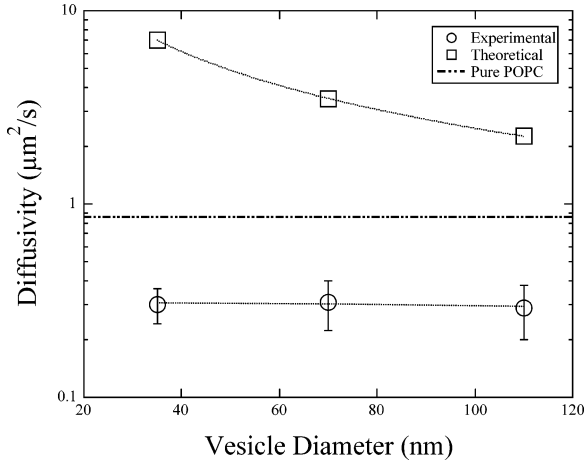

Figure 5. Plot of diffusivity versus the diameter of the vesicles tethered to the supported lipid bilayer via hybridized cholesterol−DNA. The circles indicate the experimental data, and the squares represent calculated diffusion coefficients for free vesicles in water. The dashed line is set at the value for the diffusivity of the lipid molecules within the bilayer.

cholesterol at the 3′ end was then added to the free vesicles. This strand was complementary to the remaining 15 mers at the unlabeled end of the 30-mer DNA. With the hybridized DNA oriented so that the double cholesterol end was embedded within the SPB, the diffusion coefficient for the tethered vesicles decreased by a factor of 3, as shown in Figure 6.

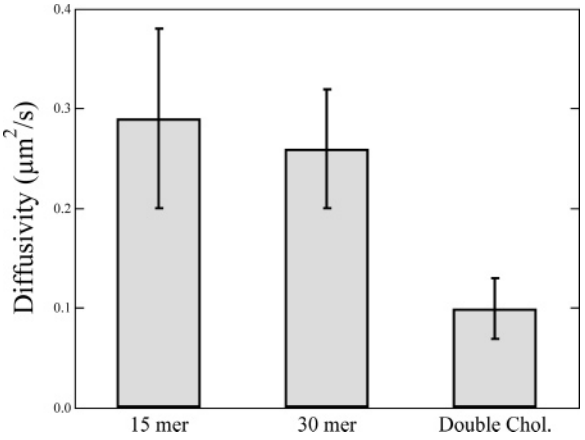

Figure 6. Comparison of the diffusion coefficient for 110 nm vesicles tethered by $cDNA_{15}/cDNA_{15}'$ (15 mer), $cDNA_{30}/cDNA_{30}'$ (30 mer), and $cDNA_{30}'/dcDNA_{15}/cDNA_{15}$ (double chol.).

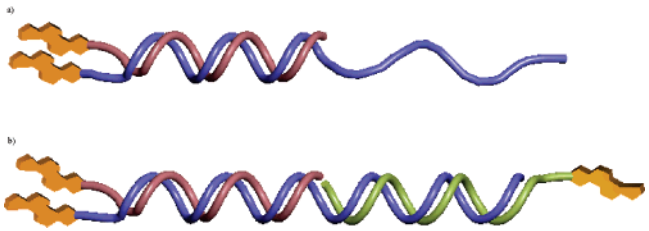

Figure 7. Schematic of (a) double cholesterol−DNA paring formed from the hybridization of $cDNA_{30}'/dcDNA_{15}$, and (b) completed tether formed when $cDNA_{13}$ hybridizes with the free end of the double cholesterol−DNA pair.

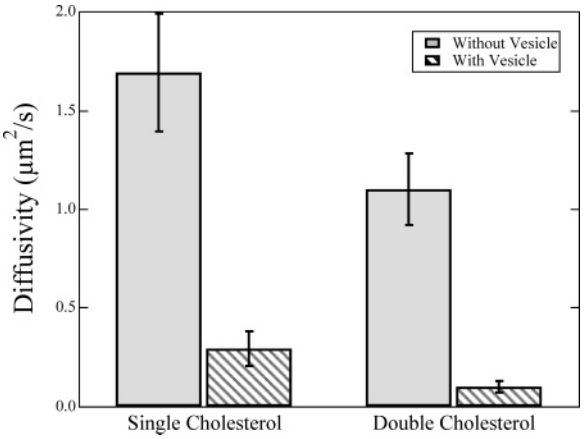

Figure 8. Comparison of cholesterol-DNA diffusivity with attached vesicles (solid bars) and without (striped bars). Both the single and double cholesterol anchors diffuse much more rapidly than the corresponding vesicle−DNA assemblies. The diffusivity of the single cholesterol anchor is 6 times faster without attached vesicles, and the double cholesterol anchor is 11 times faster.

DNA Anchors. Last, the lateral mobility of the cholesterol−DNA anchors was measured in the absence of attached vesicles. These hybrid pairs were formed from the single cholesterol anchor, $dcDNA_{30}/rDNA_{15}'$, and the double cholesterol anchor, $dcDNA_{30}/dcDNA_{15}'/rDNA_{15}'$ (Table 1). For the single cholesterol anchor, D was measured to be 1.6 $\mu m^2/s$, as shown in Figure 8. D was 1.5 times slower for the double cholesterol anchor and was equal to 1.1 $\mu m^2/s$

Observe that the tracer diffusion of the cholesterol anchors was similar to, but somewhat faster than, POPC. Moreover, the POPC value is somewhat low compared to the reported values

for lipid bilayer diffusion on glass substrates. These vary between 4 and 8 $\mu m^2/s$.[25−27] The lower value observed in these experiments may be attributed to surface defects, impurities, or strong interactions between the glass and the lipid molecules in the lower leaflet. The latter condition may cause a difference between the mobility of the upper and lower leaflets. Indeed, the use of a double exponential generally produced better fits to the experimental data. Although a faster component around 5 $\mu m^2/s$ appeared from such treatment of the data, this time constant and associated coefficient displayed unacceptably large scatter and did not appear reliable. However, based on these observations, it would not be unreasonable to suspect that the diffusion coefficient of the upper leaflet was more in line with that of the single cholesterol−DNA.

Discussion

Cholesterol-Limited Diffusion. The vesicle−DNA assembly is comprised of three parts: a vesicle, a DNA tether, and a cholesterol anchor. One might hypothesize that the lateral mobility of the assembly is limited by the slowest moving component. The FRAP measurements indicated that the diffusivity of vesicle−DNA assemblies was sensitive neither to the size of the vesicle nor to the length of the DNA tether. However, they also showed a decrease in diffusivity by a factor of 3 when the size of the hydrophobic anchor was increased from one to two cholesterols.

Given that the lateral mobility depends only on anchor size, the cholesterol in the bilayer must therefore diffuse significantly more slowly than the attached vesicles. In this case, cholesterol−DNA diffusion occurs between 1.1 and 1.6 $\mu m^2/s$, whereas the free vesicles in water would diffuse between 2 and 7 $\mu m^2/s$. This difference appears to be large enough so that the effects of viscous drag on the vesicles can be ignored. For larger vesicles, it is not clear whether this assumption is still valid. Either the overall diffusivity will be determined by the additive effects of viscous drag on each component or it will be limited by the diffusion rate of the slowest component. For the current range of tether lengths and vesicles sizes, the latter appears to be true.

Multiple Anchors. Contradicting the notion that cholesterol alone controls the mobility is the fact that single cholesterol−DNA and double cholesterol−DNA have a diffusivity 6 and 11 times faster, respectively, than their corresponding tethered vesicle assemblies. This discrepancy can be explained by the fact that each vesicle can be tethered to the bilayer by multiple DNA tethers. We can make a rough estimate of the DNA:vesicle molar ratio by making a few assumptions about the POPC vesicles. Given a lipid molecular weight of 760.09 g/mol, a bilayer thickness of about 5 nm,[28] an area per lipid headgroup of about 0.7 nm,[2,29] and a lipid concentration of 0.2 mg/mL, we arrive at an approximate concentration of 6 nM for the 35 nm vesicles and 0.6 nM for 110 nm vesicles. These compare to a 60 nM concentration of cholesterol−DNA. Accordingly, the average number of DNA molecules decorating each vesicle is about 10 for the 35 nm vesicles and 100 for the 110 nm vesicles.

Although many DNA strands are available for hybridization, the number of active contact points between the vesicle and SPB is almost certainly lower. This possibility is illustrated in Figure 9. The first limiting factor is that many cholesterol−DNA strands remain unhybridized. Another mitigating factor is the tendency of the cholesterol to exchange in and out of the bilayer. The recent work of Pfeiffer and Höök showed that single cholesterol−DNA strands desorb from SPBs with a rate constant of 6×10^{-4} s^{-1}, whereas double cholesterol−DNA appeared to be irreversibly anchored.[24] It is therefore likely that the number of DNA tethers anchored via one cholesterol moiety is slowly reduced over time.

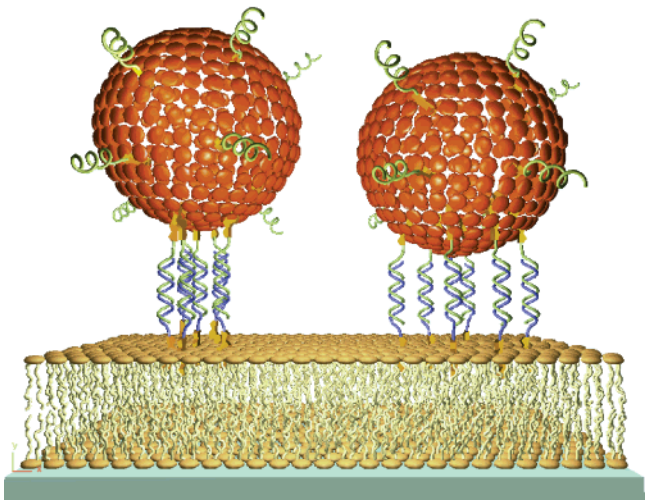

Figure 9. Schematic of possible vesicle−DNA assembly configuration. As many as 100 cholesterol−DNA molecules may decorate the exterior of the vesicles. Of these molecules, only a fraction may be able to hybridize with the complementary cholestero−-DNA strands on the SPB surface. The number of active tethers between the vescicle and SPB may be limited by the surface concentration of cholesterol-DNA or by the effective contact area. As shown in the figure, the DNA tethers can increase the effective contact area by moving out toward the perimeter in a crown-like configuration. In doing so, tethers bring the vesicle closer to the SPB but also create extra lateral spacing. The finite lifetime of cholesterol−DNA adsorption means that this picture can become more complicated as the cholesterol anchors exchange in and out of the bilayer.

Perhaps the most important factor is the effective contact area between the vesicles and the SPB. Although the proximity of the vesicle to the surface facilitates additional hybridization with surface-bound DNA, the tethers will tend to repel one another due to electrostatic repulsion. The decay length of DNA−DNA repulsion is difficult to calculate. However, the equation of state for long DNA pairs has been measured as a function of applied osmotic stress. These measurements indicated a decay length of $4\lambda_D$ in the range of roughly 4−12 nm spacing, where λ_D is the Debye length.[30] For a 100 mM NaCl buffer, the repulsion decays after 4 nm. This distance compares to an effective contact diameter of 6.5 nm for 35 nm vesicles and 11.5 nm for the 110 nm vesicles, where the effective contact diameters are estimated as the diameters over which water molecules, of diameter 0.3 nm,[31] are excluded between the spherical vesicles and planar SPB. Now consider what happens if the tethers spread out around the perimeter of the contact area. This crown-like configuration not only allows a rapid increase in the effective contact area but it also allows a small degree of freedom normal to the bilayer surface (Figure 9). One can perhaps picture a situation where movement of the vesicle in the z direction is accompanied by radial displacement of the DNA tethers. Since vesicle deformation and other perturbations would increase the effective contact area even further, the vesicle−DNA assemblies can clearly accommodate more than a single tether.

One can more accurately estimate this number (N) by comparing the diffusivity of the vesicle assemblies to that of the cholesterol−DNA by itself. To perform such a calculation, one must choose between either a free draining model or a unit aggregate diffusion model. In the free draining limit where the cholesterol moieties diffuse in the bilayer unperturbed by other cholesterol−DNA linked to the vesicle, the diffusivity is

inversely proportional to N.[32,33] Since the diffusion coefficient of the single cholesterol assemblies was 6 times lower than that of the individual anchors, one would estimate 6 active tethers per vesicle, regardless of vesicle size.

One can also consider the unit aggregate limit, where the cluster of cholesterol moieties can be treated as a solid cylinder of radius R_c and height h. The translational diffusion coefficient of such an aggregate in a viscous lipid layer of thickness h and viscosity η is[33−35]

$$D = (k_B T/4\pi\eta h) \log[(\eta h/\eta' R_c) - \gamma] \quad (5)$$

where η' is the viscosity of water, and γ is Euler's constant, equal to 0.5772. Here one sees a much weaker dependence on the number of cholesterol anchors, noting that R_c scales as the square root of N. The scaling of the diffusion coefficient therefore follows a $\log[N^{-1/2} - \gamma]$ dependence. Although the cholesterol anchor does not fully span the bilayer, this model provides guidance for what can be expected. It predicts a weak dependence on the number of anchor points, but it would still be significant when going from 35 to 110 nm vesicles if the number of tethers was actually proportional to the molar ratio between the vesicles and cholesterol-DNA.

Fixed Number of Anchors. Since both diffusivity models predict significant sensitivity to the number of anchors, it must be roughly constant for the three vesicle sizes. Given the differences in effective contact areas and the number of attached cholesterol−DNA strands, this result is surprising. To put these differences into perspective, a 110 nm vesicle is expected to have approximately 3 times as much available contact area and 10 times as many available DNA strands as a 35 nm vesicle.

This paradox would not be as difficult to reconcile if there was only one tether per vesicle. Certainly, if the number of tethers is allowed to vary, it is much harder to argue that this number is not affected by the vesicle size under our conditions. One could instead argue that a maximum of one DNA tether can be formed and that the remaining cholesterol strands on the vesicle remain unhybridized. Since the number of active tethers can be limited by kinetics, DNA−DNA repulsion, geometric constraint, and other factors, this possibility cannot be ruled out.

The problem with this interpretation is that it does not explain why the tethered vesicle assemblies diffuse so much more slowly than the tethers by themselves. Neither does it explain why this relative decrease in diffusivity is different for single cholesterol−DNA than it is for double cholesterol−DNA. Furthermore, single cholesterol−DNA tethers are not expected to remain for long periods on the bilayer surface. According to ref 24, they have a residence time of only 30 min. This lifetime compares to the 5 h that were typically needed to perform multiple FRAP measurements on a single sample. Although no direct measurement has been made to rule out the possibility of having a single tether per vesicle, it appears unlikely based on numerous observations in these experiments.

A key variable is the areal density of tethered assemblies. As stated earlier, this value was held constant for a given sample by observing areas that gave the same autoexposure time. This guideline may have inadvertently restricted our observations to areas where the number of tethers per vesicle was fixed at some arbitrary number. Two rates must be considered: the rate of forming the first tether and the rate of hybridizing additional DNA pairs after the first tether has formed. If the latter is rapid compared to the former, then the first vesicles to reach the surface will possess the largest number of tethers. They will also deplete the surface-bound DNA, preventing additional vesicles from coupling to the SPB. The local concentration of surface-bound DNA would then determine both the areal density of tethered vesicles and the number of tethers per vesicle. For those areas with the same fluorescence intensity, the local surface coverage of DNA may have limited each vesicle to a fixed number of tethers, regardless of vesicle size.

We also note that the areal density of assemblies has to increase with decreasing vesicle size in order to maintain the same fluorescence intensity. Since the mean free path of the vesicles can affect the diffusion rate, it is possible that the surface coverage was in a regime where this variable also had an impact on the data. A more thorough investigation of the effects of assembly coverage and DNA concentration that would be required to reach a definite conclusion is beyond the scope of the present work, and it will be postponed to future studies.

Single vs Double. Next we consider the decrease in D caused by using double cholesterol anchors rather than single cholesterol. The first question is whether the cholesterol pair diffuses as a single unit or whether they can be modeled as a two beads connected by a spring. If the latter is true, then the free draining limit states that D for single cholesterol−DNA should be a factor of 2 larger than for double cholesterol−DNA. The actual ratio was 1.5. Although this ratio is not large enough to conclude that the two cholesterol molecules diffuse independently, it is nearly a factor of 2 within the experimental error.

If each vesicle was tethered by only a single DNA pair, then one would expect that the assemblies with single cholesterol−DNA would have a diffusivity 1.5 times greater than the corresponding double cholesterol assemblies. The actual factor is closer to 3. This discrepancy can again be explained in terms of the number of active tethers per vesicle. Consider the concentration of cholesterol−DNA for both the single and double cholesterol−DNA at the beginning of the experiment. Equal amounts are initially added to the sample volume. However, the affinity constant ($1/K_d$) for the double cholesterol−DNA is at least an order of magnitude greater than that for the single cholesterol−DNA.[24] The resulting improvement in uptake therefore leads to a higher surface concentration throughout the experiment. Based on this argument, the number of active tethers per vesicle should also be higher. We can again invoke the free draining limit where the individual anchors diffuse independently but are connected by a restoring force. By comparing D for the assemblies to that of the anchors alone, we estimate that there are approximately 6 active tethers per vesicle when single cholesterol-DNA is used, and 11 active tethers per vesicle when double cholesterol-DNA is used.

Conclusions

The diffusivity of the tethered vesicle−DNA assemblies is neither sensitive to the size of the attached vesicles nor to the length of the DNA tether. However, changing the hydrophobic anchor size from one cholesterol moiety to two results in a decrease of the diffusivity by a factor of 3. The strong influence of the anchor size suggests that the lateral mobility of the assemblies is controlled by the diffusion of cholesterol in the SPB. Perhaps even more notable is the fact that single cholesterol anchors without vesicles are found to diffuse 6 times faster than the corresponding vesicle assemblies. This discrepancy is believed to arise from the fact that each vesicle is tethered to the bilayer by multiple DNA tethers. If we assume that the cholesterol groups diffuse according to the free draining limit, then we can estimate approximately 6 tethers per vesicle for the single cholesterol−DNA and 11 tethers per vesicle for the double cholesterol−DNA under our experimental conditions.

Acknowledgment. J. J. B. thanks the N.S.F. for providing him with the MPS/DRF Distinguished International Postdoctoral Fellowship under Award Number DMR-0301195. He also thanks Indriati Pfeiffer, Angelica Wikström, and Nina Tymchenko for their advice and training. Partial support was also provided by the Biomimetic Material Science Program funded by the Swedish Foundation for Strategic Research (SSF).

References and Notes

(1) Ziegler, C.; Göpel, W. *Curr. Opp. Chem. Biol.* **1998**, *2*, 585.
(2) Stelzle, M.; Weissmüller, G.; Sackmann, E. *J. Phys. Chem.* **1993**, *97*, 2974.
(3) Svedhem, S.; Pheiffer, I.; Larsson, C.; Wingren, C.; Borrebaeck, C.; Höök, F. *ChemBioChem* **2003**, *4*, 339.
(4) Granéli, A.; Rydström, J.; Kasemo, B.; Höök, F. *Langmuir* **2003**, *19*, 842.
(5) Cornell, B. A.; Braach-Maksvytis, V. L. B.; King, L. G.; Osman, P. D. J.; Raguse, B.; Wieczorek, L.; Pace, R. J. *Nature* **1997**, *387*, 580.
(6) Keller, C. A.; Kasemo, B. *Biophys. J.* **1998**, *75*, 1397.
(7) Salamon, Z.; Huang, D.; Cramer, W. A.; Tollin, G. *Biophys. J.* **1998**, *75*, 1874.
(8) Schouten, S.; Stroeve, P.; Longo, M. L. *Langmuir* **1999**, *15*, 8133.
(9) Salafsky, J.; Groves, J. T.; Boxer, S. G. *Biochemistry* **1996**, *35*, 14773.
(10) Gizeli, E.; Lowe, C. R.; Liley, M.; Vogel, H. *Sens. Actuators, B* **1996**, *34*, 295.
(11) Helm, C. A.; Israelachvili, J. N.; McCuiggan, P. M. *Science* **1989**, *246*, 919.
(12) Zäch, M.; Kasemo, B., *Proc. AIP* **2003**, *CP696*, 447−451.
(13) Salafsky, J.; Groves, J. T.; Boxer, S. G. *Biochemistry* **1996**, *35*, 14773.
(14) Sackmann, E.; Tanaka, M. *Tibtech* **2000**, *18*, 58.
(15) Naumann, R.; Baumgart, T.; Gräber, P.; Jonczyk, A.; Offenhäuser, A.; Knoll, W. *Biosens. Bioelectron.* **1997**, *17*, 25.
(16) Richard, P.; Rigaud, J.-L., Gräber, P. *Eur. J. Biochem.* **1990**, *193*, 921.
(17) Yoshina-Ishii, C.; Boxer, S. G. *J. Am. Chem. Soc.* **2003**, *125*, 3696.
(18) Patolksy, F.; Katz, E.; Bardea, A.; Willner, I. *Langmuir* **1999**, *15*, 3703.
(19) MacDonald, R. C.; MacDonald, R. I.; Menco, B. P. M.; Takeshita, K.; Subbarao, N. K.; Hu, L.-R. *Biochim. Biophys. Acta* **1991**, *1061*, 297.
(20) Axelrod, D.; Koppel, D. E.; Schlessinger, J.; Elson, E.; Webb, W. W. *Biophys. J.* **1976**, *16*, 1055.
(21) Ross, J. L.; Fygenson, D. K. *Biophys. J.* **2003**, *84*, 3959.
(22) Einstein, A. *Investigations of the Theory of Brownian Movement*; Fürth, R., Ed.; Dover: New York, 1956; 36−67.
(23) Weast, R. C., et al., Ed.; *CRC Handbook of Chemistry and Physics*, 69th ed.; CRC Press: Boca Raton, FL, 1989; F-40.
(24) Pfeiffer, I.; Höök, F. *J. Am. Chem. Soc.* **2004**, *126*, 10224.
(25) Salafsky, J.; Groves, J. T.; Boxer, S. G. *Biochemistry* **1996**, *35*, 14773.
(26) Stelzle, M.; Miehlich, R.; Sackmann, E. *Biophys. J.* **1992**, *63*, 1346.
(27) Groves, J. T.; Boxer, S. G. *Biophys. J.* **1995**, *69*, 1972.
(28) Salamon, Z.; Tollin, G. *Biophys. J.* **2001**, *80*, 1557.
(29) Gennis, R. B. In *Biomembranes*; Cantor, C. R., Ed.; Springer-Verlag: New York, 1989.
(30) Strey, H. H.; Parsegian, V. A.; Podgornik, R. *Phys. Rev. Lett.* **1997**, *78*, 895.
(31) Franks, F. *Water: 2nd ed.; A matrix of life*; Royal Society of Chemistry: Cambridge, 2000.
(32) Flory, P. J. *Principles of Polymer Chemistry*; Cornell University Press: Ithaca, NY, 1953.
(33) Kucik, D. F.; Elson, E. L.; Sheetz, M. P. *Biophys. J.* **1999**, *76*, 314.
(34) Saffman, P. G.; Delbrück, M. *Proc. Natl. Acad. Sci.* **1975**, *72*, 3111.
(35) Saffman, P. G. *J. Fluid Mech.* **1976**, *73*, 593.